12WCEE 2000

THREE-DIMENSIONAL BEHAVIORS OF REINFORCED CONCRETE BEAM-COLUMN JOINT UNDER SEISMIC LOAD

Yoshimasa OWADA[1]

SUMMARY

Two specimens tested by the author were analyzed by the non-linear three-dimensional finite element method. On specimen, ***JO-5*** was without lateral beam, and the other specimen, ***JXY-3*** was with lateral beams on both sides of joint panel. The shear reinforcements did not provided in the joint panel of both specimens. Both specimens failed due to shear at joint panel in the test.

In this finite element analysis, the orthotoropic rectangular prism element with eight nodes is used as concrete. The stress strain relationship of the joint concrete of specimen ***JXY-3***, column and beam core concrete is considered to the tri-axial confining effect, while the joint concrete of ***JO-5*** without lateral beams and covered concrete of beams and columns are assumed to uni-axial stress conditions. Stringer element is used as steel reinforcement and the bi-linear stress strain relationship is assumed. Linkage element is used as bond and two types of relationship between bond stress and slip are assumed according to the location of bond links.

The analyzed ultimate shear strengths, ductilities and final failure modes of both specimens agreed well with the test results. It was confirmed that the ultimate shear strength of joint panel was decided by the compressive failure of strut concrete, and the principal compressive stress distribution in the center layer of joint panel was different from the surface layer of joint core and covered layer.

INTRODUCTION

The objective of this study was to make clear the three-dimensional behaviors of reinforced concrete interior beam-column joints subjected to seismic load. For this purpose two beam-column joints with and without lateral beams were analyzed by the non-linear three-dimensional finite element method, and the ultimate shear strength, the failure mechanism and the stress distributions in the joint panels were mainly discussed.

2. OUTLINE OF TEST AND TEST RESULTS

2.1 Outline of Test

Two 1/4 scale cruciform models were made of subassemblages from lower story of a reinforced concrete building as shown in **Fig. 1.** The isolated joint, ***JO-5*** consisted of two 12cm by 20cm beams and a 15cm by 15cm

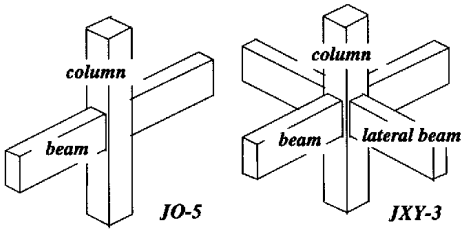

Fig. 1: Type of Test Specimen

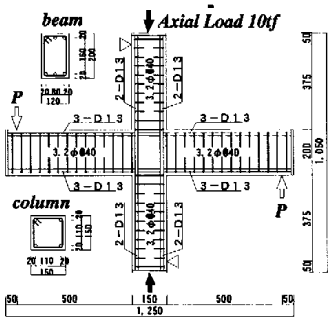

Fig. 2: Details of Specimen

[1] *Shiibaura Institute of Technology e-mail: owada@sic.shibaura-it.ac.jp*

lateral beams on both sides of the beam-column joint. The main longitudinal reinforcement of beams and lateral beams consisted of 3-D13 reinforcing bars at the both top and bottom. The column was reinforced longitudinally by 4-D13 bars. Beams, lateral beams and columns were provided 3.2mm stirrups and hoops spaced 40mm, respectively. On the other hand the beam-column joints of both specimens were not placed shear reinforcements. Design details of test specimen and properties of concrete and reinforcing bars are shown in **Fig. 2** and **Table 1**, respectively.

Alternative cyclic loads were applied at the beam tips by two oil jacks, but the transverse beams were not applied any loads. The compressive axial load (σ=66.7*kgf/cm*^{2}) was applied at the top of column by an oil jack, and was kept constant through the test. Story drift was measured with linear differential transformers (LVDT's) attached on beam tips. Joint shear deformations of the specimens ***JO-5*** and ***JXY-3*** were measured with LVDT's attached at the joint panel and the transverse beam end, respectively. The strains of longitudinal reinforcements and concrete were measured by wire strain gages.

2.2 Test Results

Fig. 3 shows final crack patterns at beam-column joints of both specimens.

In case of specimen ***JO-5***, diagonal shear cracks occurred on the joint panel at the first loading cycle, and many shear cracks developed in whole region of joint and those widths extended during testing. The covered concrete of joint region crashed and spalled off at following large deflection loading cycles. This specimen failed due to joint shear without beam and/or column yielding. In case of ***JXY-3***, shear cracks developed toward four sides of lateral beam end, however their lengths and widths were not so significant in comparison to ***JO-5***. The final failure of this specimen was joint shear failure after column yielding.

Table 1: Properties of Materials

(a) concrete

compressive strength f_c (*kgf/cm*^{2})	tensile strength f_{sp} (*kgf/cm*^{2})	Young's modulus E_c (*kgf/cm*^{2})	compressive strain ε (%)
383	33.9	2.46×10^5	0.2

(b) steel

	sectional area A (*cm*^{2})	yield strength f_y (*kgf/cm*^{2})	tensile strength f_t (*kgf/cm*^{2})	*elongation* ε (%)
D10	0.713	3560	5330	20.8
3.2ϕ	0.080	5330	4940	10.3

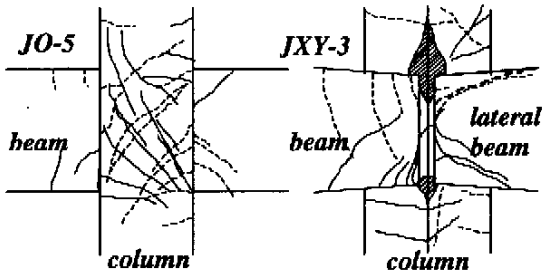

Fig. 3: Final Crack Pattern

Table 2: Test Results

	joint shear cracking		ultimate joint shear		ultimate strength	failure mode
	v_{jc} (*kgf/cm*^{2})	v_{jc}/f_c	v_{ju} (*kgf/cm*^{2})	v_{ju}/f_c	v_u/v_{ucal}*	
JO-5	44.0	0.115	105.0	0.274	0.85	joint shear failure
JXY-3	88.0	0.230	129.5	0.338	1.05	joint shear failure after column yielding

v_{ucal} : ultimate flexure strength calculated by e-function method

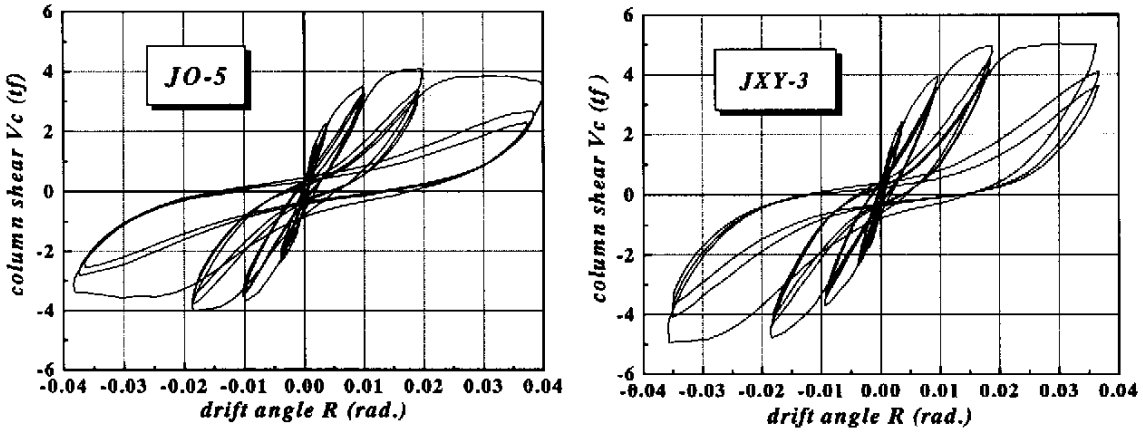

Fig. 4: Column Shear vs. Drift Angle Curve

As shown in **Table 2**, the joint shear cracking stresses v_{jc} of specimens ***JO-5*** and ***JXY-3*** were 44kgf/cm^2 and 88kgf/cm^2, and the ratio of v_{jc} to the compressive strength of concrete f_c were 0.115 and 0.23, respectively. The ultimate joint shear stresses v_{ju} of both specimens were 105*kgf/cm*^{2} and 130*kgf/cm*^{2}, and the ratios of v_{ju} to f_c were 0.27 and 0.34, respectively. Ultimate strength of ***JXY-3*** was 24% higher than that of ***JO-5*** due to the confinement effect of the joint panel by the transverse beams.

Fig. 4 shows the relations between applied column shear *Vc* and story drift angle *R* obtained from both specimens. They indicated the pinched shape and were similar to each other. In case of specimen ***JO-5***, the peak load at large displacement cycles decreased into about 90% of the maximum load due to joint shear failure, while in case of ***JXY-3***, the reduction of strength did not occur through the test.

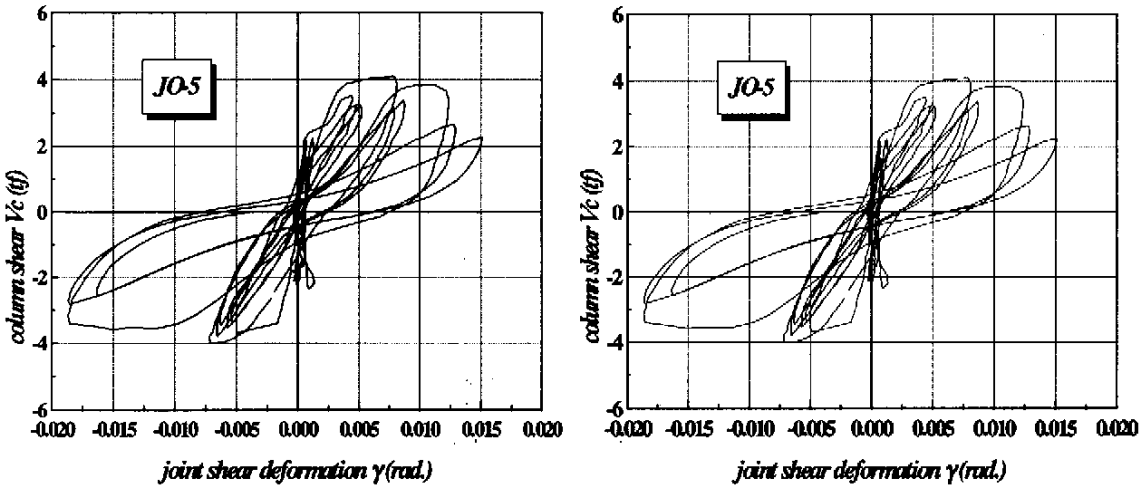

Fig. 5: Story Shear vs. Joint Shear Deformation Curve

The relations between applied column shear *Vc* and shear deformation γ are shown in **Fig. 5**. The shear deformations of ***JO-5*** and ***JXY-3*** were measured at the surface of the joint panel and the end surface of lateral beam. They increased according with the loading cycle increased, and reached almost 0.02 in negative cycle of ***JO-5*** and 0.01 in positive cycle of ***JXY-3***, respectively, because these specimens finally failed due to joint shear.

3. ANALYTICAL METHOD

The specimens ***JO-5*** and ***JXY-3*** are analyzed by the non-linear three-dimensional finite element method. The finite element idealization of the specimen ***JO-5*** shows in **Fig. 6**. The idealization of the lateral beams of ***JXY-3*** is identical of the beams of ***JO-5***. In this finite element analysis, the orthotropic rectangular prism element with eight nodes is used as the concrete element. The stringer elements as the longitudinal bars and the shear reinforcements, the linkage element as the bond are used, respectively. The incremental loads are applied at the column tips in this analysis, while the loads are applied at the beams in the test. The column axial load is kept constant. The stress strain relationships of concrete, steel reinforcement and bond link are as follows:

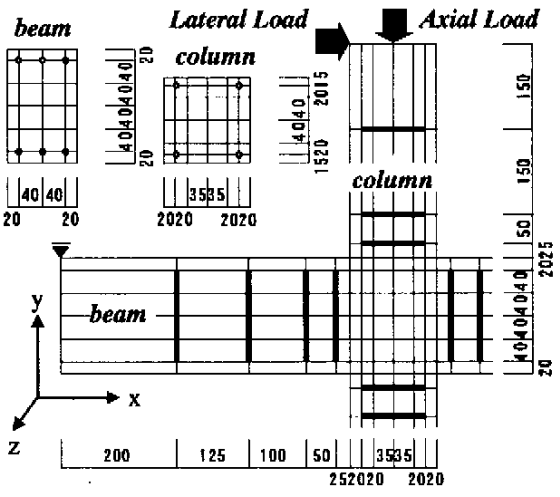

Fig. 6: Finite Element Idealization

3.1 Concrete

The joint concrete of specimen ***JO-5*** without hoops and covered concrete of beams and columns are not confined, so that the stress strain relationship is

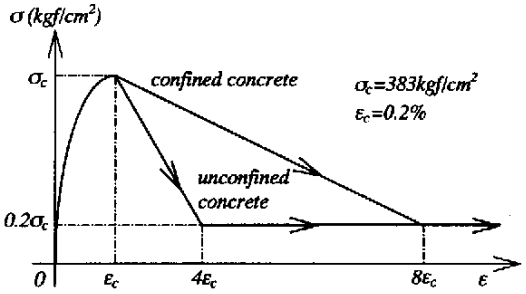

Fig. 7: Stress Strain Curve of Compressive Concrete

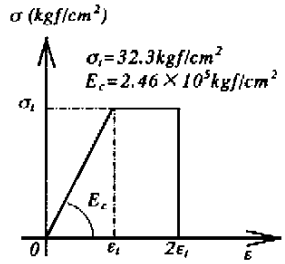

Fig. 8: Stress Strain Curve of Tensile Concrete

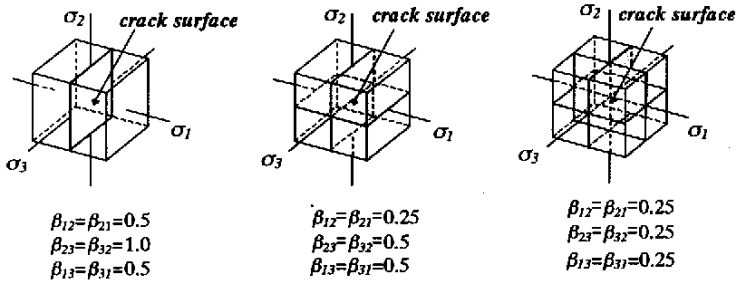

Fig. 9: Reduction Factor for Shear Rigidity

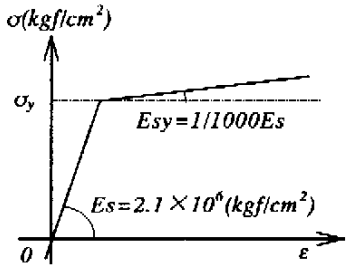

Fig. 10: Stress Strain Curve of Longitudinal Reinforcement

assumed to be uniaxial stress conditions. On the other hand, the joint concrete of ***JXY-3*** with lateral beams on both sides of the joint regards as confined concrete, and tri-axial confining effect is considered. The core concrete of beams and columns is also considered as confined concrete. The relationship between stress and strain in compression stage is followed the equivalent uni-axial stress strain model by Saenz before compressive yielding as shown in **Fig. 7**. After yielding, it is assumed that the strains of unconfined and confined concrete increase to $4\varepsilon_c$ and $8\varepsilon_c$, respectively, while the stresses of them decrease to $0.2\sigma_c$ and keep this value after then. The Draker-Prager model is used as the failure criteria for concrete.

In this analysis, the smeared crack model is used. As shown in **Fig. 8**, it is assumed that the crack occurs if the principal strain of the center of element exceeds to twice time of ε_t, and then the cracking element did not carry the tension stress normal to the crack surface.

The shear transfer along cracks surface is essentially depend on the crack width, although in this analysis, it is assumed that the shear rigidity of the cracked element decrease according to the number of crack surface, as shown in **Fig. 9**. Namely, the reduction factor of shear rigidity β becomes 0.5 for element with one cracked surface and 0.25 for that with two cracked surfaces.

3.2 Steel Reinforcement

The bi-linear stress strain relationship is used for longitudinal reinforcement and shear reinforcement, as shown in **Fig. 10**. It is assumed that the stiffness after yielding E_y becomes 1/1000 of the initial stiffness E_s.

3.3 Bond

Two types of relationship between bond stress τ_b and slip s of longitudinal reinforcement are used in this analysis according to the location of bond links. The bond yield strength τ_{by} of beam reinforcements in the joint area is assumed two times of exterior parts of the joint area because of confinement by the column axial load. In case of the bond slip relationship for beam reinforcements in the joint region, slip s exceeds that of yield strength s_y, then τ_b decreases to $1/2\tau_{by}$ and keeps constant after yield. The shear cracks occur in the joint panel before yielding of bond, then the bond stiffness connected to the cracked element is reduced to 1% of the initial stiffness K_b, and τ_b is reduced to τ_{bs} as shown in **Fig. 11(a)**. While in cases of beam reinforcements of exterior region of the joint area and column reinforcements, the slip s exceeds s_y, then τ_{by} is reduced to $1/2\tau_{by}$, and τ_b and K_{by} are reduced due to bi-axial cracking along the longitudinal reinforcement, as shown in **Fig. 11(b)**.

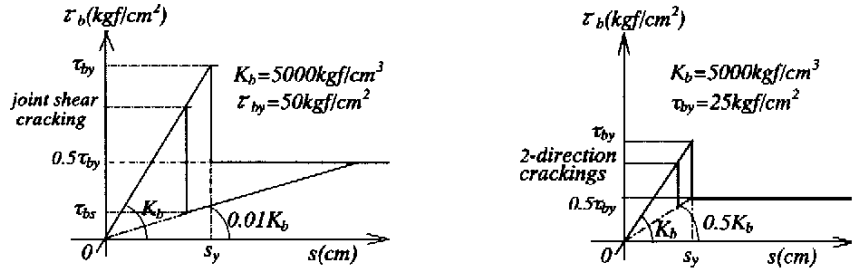

(a) beam reinforcement in joint region **(b) another reinforcements**

Fig. 11: Bond Stress vs. Slip Relationship of Longitudinal Reinforcement

4. ANALYTICAL RESULTS AND DISCUSSIONS

4.1 Relationships between Story Shear and Drift Angle

The comparisons of the calculated relationships between column shear V_c and drift angle R with the experimental results of specimens ***JO-5*** and ***JXY-3*** are shown in **Figs. 12(a) and (b)**, respectively. The calculated ultimate joint shear strengths of both specimens agreed well with experimental results. The shear cracking strengths obtained from this analysis agreed approximately with the test results. The calculated initial stiffness of ***JO-5*** and that of ***JXY-3*** agreed well with the test results, while they were estimated higher than the experimental values after joint shear cracking.

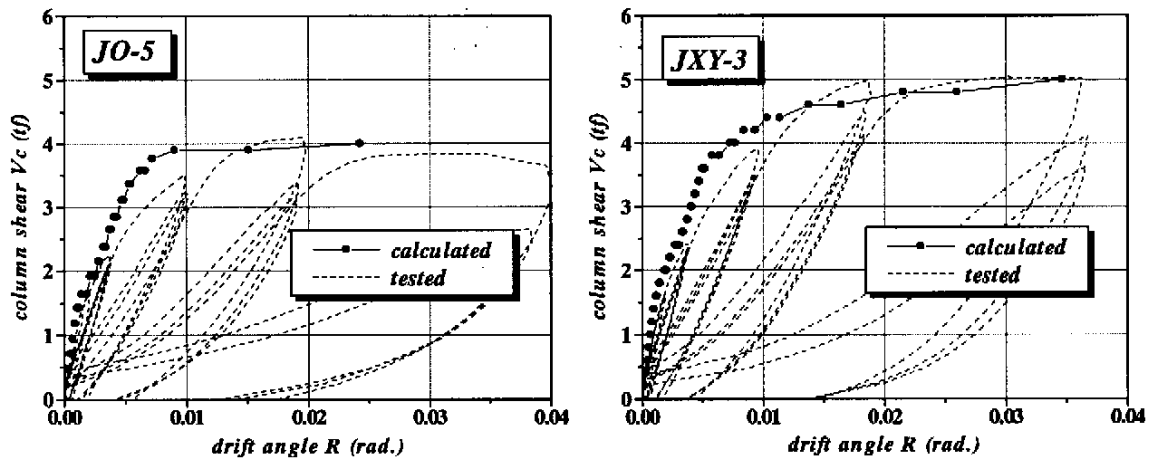

(a) JO-5 **(b) JXY-3**

Fig. 12: Comparison of Column Shear vs. Drift Angle Curve

4.3 Failure Patterns and Principle Stress Distributions

Fig. 13 shows the failure patterns and principal stress distributions at the joint panel of the specimens ***JO-5*** and ***JXY-3***, respectively. The principal stress is normalized as the compressive strength of concrete f_c. In this figure, core, surface and cover represent the layers of the center of the joint core, surface of the joint core and the cover concrete of the joint, respectively.

In case of ***JO-5*** without lateral beams, the failure patterns and stress distributions were almost identical between each layer of the joint panel. The ultimate strength of this specimen was decided by the compression failure at the strut ends.

In case of ***JXY-3*** with lateral beams, the failure patterns and stress distributions at the joint panel were different from each other.

The principal stress distribution of ***JXY-3*** with simple gradation is also shown in **Fig. 14.** At the column shear V_c=4.2tf, the principal stress of the center layer did not reach the compressive strength of concrete f_c, while the

principal stresses of the surface and cover layer began to exceed f_c at the ends of the compressive strut. At V_c=4.4tf, the principal stress exceeded f_c in the center layer, and it exceeded two times of f_c in the surface layer. At the following incremental loading step, V_c=4.6tf, the principal stresses of the strut in each layer exceeded f_c. At the ultimate strength stage, V_c=4.8tf, the compressive strut in the center layer diminished due to shear failure. While the compressive struts at the surface layer and cover layer developed to almost whole region of the joint

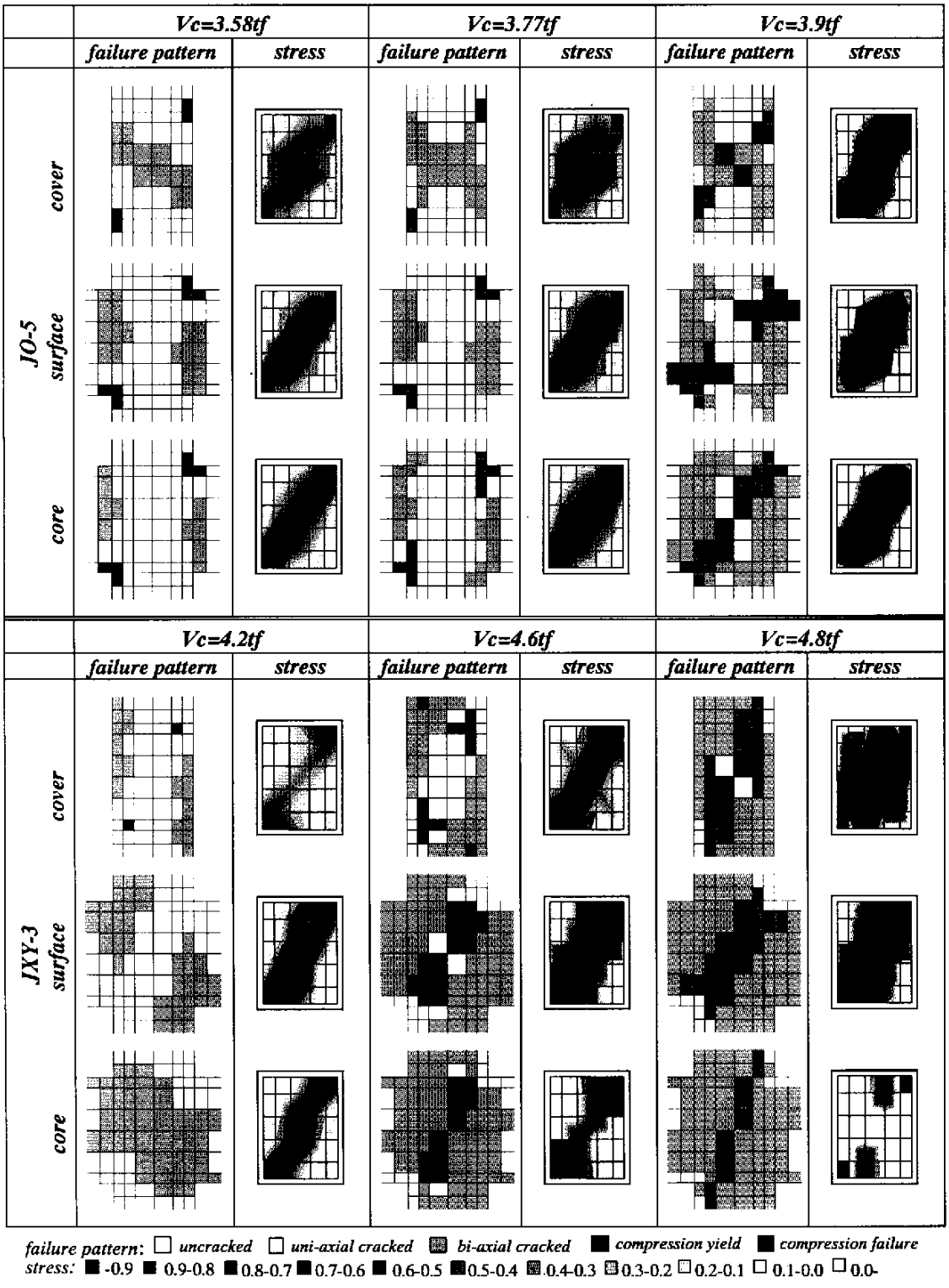

Fig. 13: Failure Pattern and Principal Stress Distribution

panel, and the principal stress exceeded f_c or $2f_c$ due to the confinement of the lateral beams.

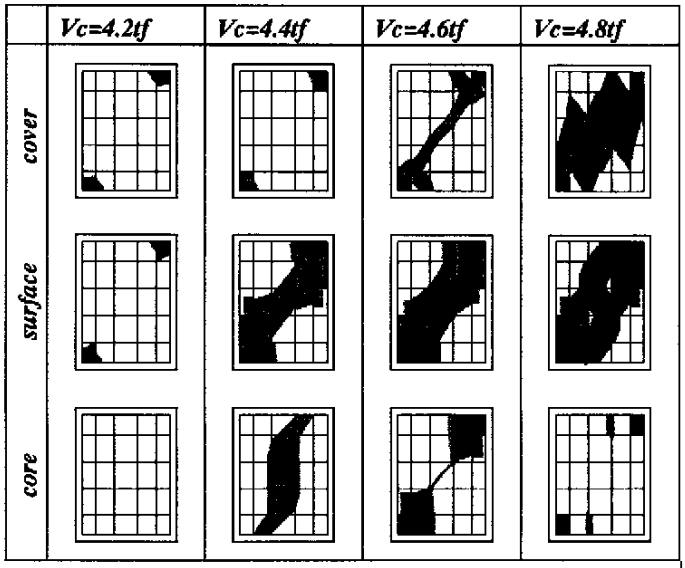

Fig. 14: Principal Stress Distributions of *JXY-3*

4.2 Relationships between Story Shear and Joint Shear Deformation

Figs. 15(a) and **(b)** show the comparisons of the calculated column shear V_c vs. joint deformation angle γ curves with tested curves of both specimens. As shown in these figures, two calculated curves were indicated that one was the shear deformation calculated at the center layer of the joint panel, the other was that of the surface layer of the joint panel in ***JO-5*** or four sides of the lateral beam end in ***JXY-3***. In the specimen ***Jo-5***, the both calculated curves agreed well the tested curve, so that the failing behaviors in the joint panel were almost identical at the surface layer and center layer. While in the specimen ***JXY-3***, the calculated shear deformations were overestimated for the tested value, especially these differences became large after the joint shear cracks developed toward four sides of lateral beams. The shear deformation calculated at the center layer was larger than that at the lateral beam end layer, so that the failing behaviors at the center layer was severe in comparison with those at the surface layer.

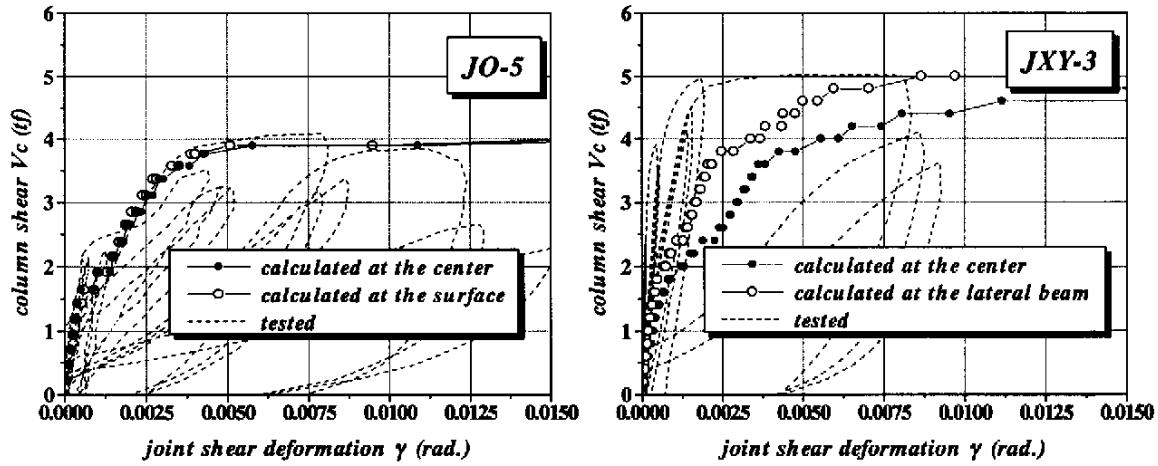

(a) JO-5 (b) JXY-3

Fig. 15: Comparison of Column Shear vs. Joint Shear Deformation Curve

5. CONCLUDING REMARKS

Main findings of this study are as follows:

(1) Final failure mode of specimen ***JO-5*** was the joint shear failure, and that of ***JXY-3*** was the joint shear failure after column yielding in this test.

(2) Ultimate joint shear strengths of ***JO-5*** and ***JXY-3*** obtained from test were 0.27 and 0.34 of the compressive strength of concrete f_c, respectively, and the confining effect by lateral beams were observed in ***JXY-3***.

(3) The calculated shear strength of both specimens agreed well with the experimental results, while the stiffness of them indicated higher than the experimental values.

(4) The calculated joint shear deformation of ***JO-5*** agreed well with the experimental result, while that of ***JXY-3*** became larger than the experimental deformation after shear cracking.

(5) The failure patterns and the principal stress distributions in the center layer of the joint panel were different from those of the surface and cover layer.

6. REFERENCES

(1) CHEN. W. F. (1985) "Plasticity in Reinforced Concrete", Maruzen Co. LTD., (in Japanese)

(2) OKAMURA, H. and MAEKAWA, K. (1991) "Nonlinear Analysis and Constitutive Models of Reinforced Concrete"; Gihodo Shuppan Co., LTD., (in Japanese)

(3) OWADA, Y. (1984) "Studies on Reinforced Concrete Beam-Column Joints under Biaxial Seismic Load"; Summaries of Technical Papers of Annual Meeting , Architectural Institute of Japan, 1984.10, Vol. C-2, pp1869-1870, (in Japanese)

(4) OWADA, Y., KAWAI, T. and SUGAYA, K. (1994) "Three Dimensional Behaviors of Reinforced Concrete Beam-Column Joints under Seismic Load (Part1-Part3)"; Summaries of Technical Papers of Annual Meeting , Architectural Institute of Japan, Vol. C-2, pp557-562, (in Japanese)

(5) SUGAYA, K and OWADA, Y. (1995) "Studies on Non-linear Behaviors of Reinforced Concrete Beam-Column Joint under Seismic Load (1)"; Summaries of Technical Papers of Annual Meeting , Architectural Institute of Japan, Vol. C-2, pp139-140, (in Japanese)

(6) SUGAYA, K and OWADA, Y. (1996) "Studies on Non-linear Behaviors of Reinforced Concrete Beam-Column Joint under Seismic Load (2)"; Summaries of Technical Papers of Annual Meeting , Architectural Institute of Japan, Vol. C-2, pp669-70, (in Japanese)